ELSEVIER

Chemical Engineering Journal 138 (2008) 179–186

Chemical Engineering Journal

www.elsevier.com/locate/cej

Enhanced adsorption capacity of activated alumina by impregnation with alum for removal of As(V) from water

Sushree Swarupa Tripathy, Ashok M. Raichur*

Department of Materials Engineering, Indian Institute of Science, Bangalore 560012, India

Received 27 December 2006; received in revised form 23 April 2007; accepted 22 June 2007

Abstract

Alum-impregnated activated alumina (AIAA) was investigated in the present work as an adsorbent for the removal of As(V) from water by batch mode. Adsorption study at different pH values shows that the efficiency of AIAA is much higher than as such activated alumina and is suitable for treatment of drinking water. The adsorption isotherm experiments indicated that the uptake of As(V) increased with increasing As(V) concentration from 1 to 25 mg/l and followed Langmuir-type adsorption isotherm. Speciation diagram shows that in the pH range of 2.8–11.5, arsenate predominantly exists as $H_2AsO_4^-$ and $HAsO_4^{2-}$ species and hence it is presumed that these are the major species being adsorbed on the surface of AIAA. Intraparticle diffusion and kinetic studies revealed that adsorption of As(V) was due to physical adsorption as well as through intraparticle diffusion. Effect of interfering ions revealed that As(V) sorption is strongly influenced by the presence of phosphate ion. The presence of arsenic on AIAA is depicted from zeta potential measurement, scanning electron microscopy (SEM) and energy-dispersive analysis of X-ray (EDAX) mapping study. Alum-impregnated activated alumina successfully removed As(V) to below 40 ppb (within the permissible limit set by WHO) from water, when the initial concentration of As(V) is 10 mg/l.

Keywords: Adsorption; Arsenic(V); Speciation; Impregnation; Alumina; Isotherm; Kinetics; EDAX mapping

1. Introduction

Due to the carcinogenic effect of arsenic to human body, extensive research has been carried out in the past decades on removing arsenic from water. Existing methods to remove arsenic from water includes adsorption [1,2], precipitation [3], anion exchange [4], reverse osmosis, coagulation processes [5], and Donnan membrane [6]. Among these methods adsorption/co-precipitation process seems to be most promising method as it reduces arsenic up to 50 ppb in the aqueous solution. Adsorption with activated carbon [7], activated alumina [8], fly ash [9], rare earth oxides [1], and manganese green sand [10] have been used to remove arsenic from water. Iron(III) oxides have shown tremendous potential for adsorption of arsenic as these oxides have high sorption affinity toward both As(V) and As(III) species [6,11]. Granular activated alumina has been found to be a very effective adsorbent for removal of arsenic from aqueous solutions [12]. However, it works at narrow pH range (i.e. pH 5–6.5) and it has more affinity for competing ions such as fluoride, phosphate than arsenic.

Though activated alumina, activated carbon, sand and rare earth oxides have been studied widely [7,13–16,1], these are not efficient for removal of arsenic from drinking water due to the low sorption capacity and also because these adsorbents work at low pH value. In recent years, several studies have been done on impregnation of various oxides, sand, carbon, polymer, spent catalyst [17–20,6] and these have been shown to be very effective for removal of toxic metals including arsenite and arsenate. Impregnation with chemicals enhances the sorption capacity of adsorbents. It has been reported that the adsorption capacity of arsenate enhanced significantly by lanthanum impregnated silica gel and could remove arsenate up to 0.2 mmol/l [21]. Huang and Liu [17] have studied the adsorption of As(V) in which the adsorption capacity of spent catalyst was increased by coating with iron. Katsoyiannis and Zouboulis [22] have used a modified polymer material which is capable of removing up to 10 μg/l inorganic arsenic from contaminated water sources. Alum-impregnated activated alumina was previously effectively tested for removal of fluoride from drinking water [23]. The aim of the present study was to examine the ability of

* Corresponding author. Tel.: +91 80 22933238; fax: +91 80 23600472.
E-mail address: amr@materials.iisc.ernet.in (A.M. Raichur).

1385-8947/$ – see front matter © 2007 Elsevier B.V. All rights reserved.
doi:10.1016/j.cej.2007.06.028

alum-impregnated activated alumina towards removal of As(V) from drinking water. Activated alumina of high surface area has been impregnated with alum and then be used as an adsorbent in the adsorption process. Various parameters such as equilibrium isotherm, adsorption kinetics, adsorbent dose, effect of pH, interference of other ions and regeneration of adsorbent have been investigated. The Mineql+ program was used to determine the speciation of arsenate in water for the present conditions. Zeta potential measurement, scanning electron microscope, energy-dispersive analysis of X-ray study were carried out for the arsenic adsorbed alum-impregnated activated alumina.

2. Materials and methods

2.1. Materials

The chemicals used in this study were of analytical grade and double distilled water was used throughout the study. Stock solutions of As(V) were prepared by dissolving appropriate amount of $Na_2HAsO_4{\cdot}7H_2O$ (Loba Chemie, Mumbai, India) in double distilled water. All solutions for adsorption and analysis were prepared by appropriate dilution of the freshly prepared stock solution. The preparation of alum-impregnated activated alumina (AIAA) has been described in an earlier publication [23]. The analytical grade activated alumina was impregnated with alum by adding 200 ml of 5% $NaHCO_3$ and 200 ml of 1 M $Al_2(SO_4)_3{\cdot}16H_2O$ solution to 100 g of activated alumina. The pH of the solution was maintained at 3.4–3.5 by addition of 0.1N HCl. In the present study activated alumina of high surface area (250 m^2/g) was used and the alum solution remained in contact with activated alumina (AA) for 24 h at 50 °C.

2.2. Characterization of adsorbent

The adsorbent was characterized for its particle size distribution using a Malvern Zeta Sizer (Malvern Zeta-sizer Model 3000, UK). The surface area was determined by using a Quantasorb surface area measurement apparatus (Quantachrome Corp., NY). The isoelectric point of AA, AIAA and the arsenic adsorbed AIAA was determined by measurement of zeta potential of the particles using the Malvern Zeta Sizer. Scanning electron microscopy (SEM) and energy-dispersive analysis of X-ray (EDAX) were performed using a FEI SIRION (20 kV).

2.3. As(V) adsorption

Adsorption experiments were carried out in batch mode and conducted in duplicate. The experimental procedure for adsorption isotherms, adsorption at different pH values, contact time, and interference of other ions has been described in an earlier communication [1]. After the equilibration time the filtrate was analysed for As(V) using an ICP Spectrophotometer (Jobin-Yvon, France).

Table 1
Properties of activated alumina and AIAA

Properties	Activated alumina (AA)	Alum-impregnated activated alumina (AIAA)
Particle size, d_{50} (μm)	82	93
Surface area (m^2/g)	242	183
Pore volume (cm^3/g)	0.39	0.20
Isoelectric point	8.3	8.6

3. Results and discussion

3.1. Characterization of adsorbent

The BET surface area of AA and AIAA were found to be 242 and 183 m^2/g. The decrease in surface area upon impregnation may be due to the diffusion of alum particles into the pores of the AA. But previous studies for fluoride removal [23] have shown that the specific surface area of activated alumina was found to increase after impregnation with alum due to the uniform coating of $Al(OH)_3$ on the surface of activated alumina. This difference in surface area of AIAA might be observed due to the different preparation technique applied such as equilibration time and heat applied during impregnation process. The pore volume, particle size and isoelectric point of AA and AIAA are given in Table 1.

3.2. Zeta potential measurement of AA and AIAA

The plot of pH versus zeta potential (Fig. 1) in 10^{-2} M KNO_3 solution shows the zeta-potential measurement of AA and AIAA. The isoelectric point of AA and AIAA is found at pH 8.3 and 8.6, respectively. The shift in IEP value to alkaline pH and change in surface charge to higher value in case of AIAA can be attributed to the impregnation of alum on AA surface.

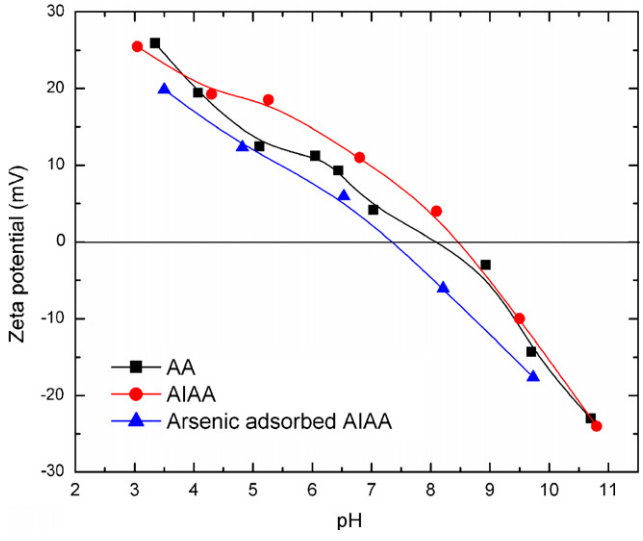

Fig. 1. Zeta potential of activated alumina, alum-impregnated activated alumina and As(V) adsorbed alum-impregnated activated alumina at an ionic strength of 0.01 M KNO_3 solution.

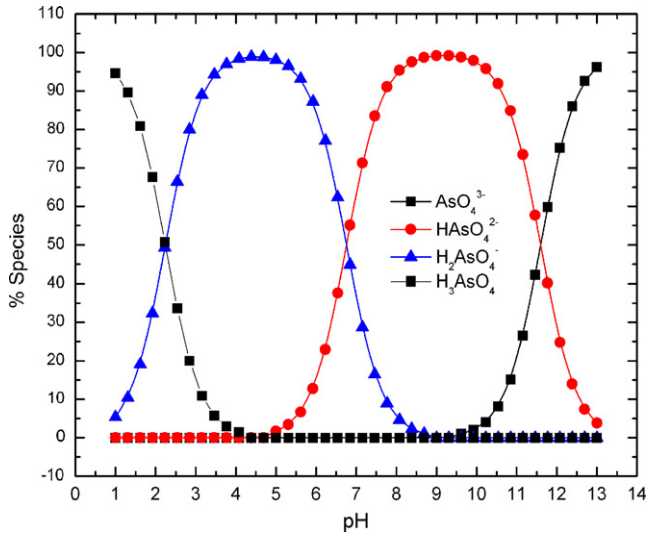

Fig. 2. Speciation diagram of arsenate.

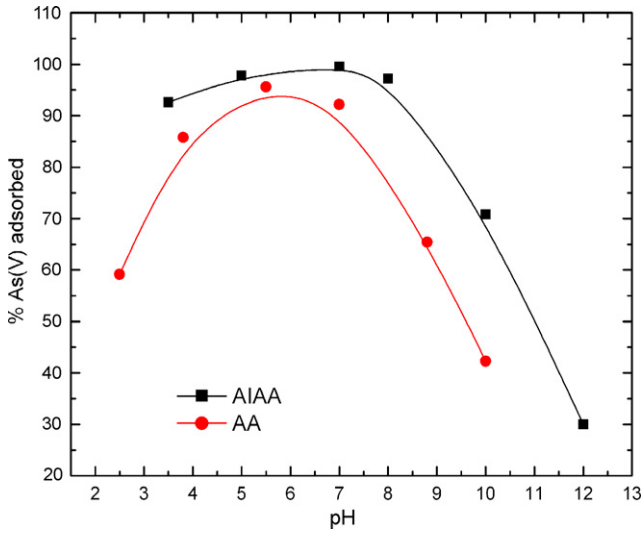

Fig. 3. The plot of percent removal of As(V) as a function of pH at adsorbent dose 8 g/l, fluoride concentration 10 mg/l and equilibrium time 3 h for AA and AIAA.

3.3. Speciation of As(V) in water

The speciation of arsenate was defined by using a well-known computer program Mineql+. According to the speciation diagram for arsenate, high percentage of $H_2AsO_4^-$ and $HAsO_4^{2-}$ species are present in the pH range 2.7–11.5 as shown in Fig. 2. Therefore, it is concluded that these species are adsorbed on the surface of AIAA during adsorption process. Mostly boehmite is formed on the alumina surface by impregnation with alum and the sorption of arsenate is as follows:

$$Al(OH)_3 + H^+ + H_2AsO_4^- \rightarrow Al(OH)_2\text{–}H_2AsO_4 + H_2O \quad (1)$$

$$Al(OH)_3 + 2H^+ + HAsO_4^{2-} \rightarrow Al(OH)\text{–}HAsO_4 + 2H_2O \quad (2)$$

3.4. Effect of pH on adsorption of As(V)

The effect of the pH on the adsorption of As(V) (10 mg/l) onto AA and AIAA was studied (Fig. 3). In case of AA, adsorption of As(V) increases rapidly with increasing pH and attained to maximum 95.6% at pH 5.5 and very low adsorption occurred at alkaline pH values. But for AIAA, adsorption is very high in the pH range of 3.5–8 and maximum adsorption of 99.6% achieved at pH 7. Thereafter adsorption dropped significantly at higher pH values and only 30% adsorption occurred at pH 12. Similar trend was observed in an earlier study on adsorption of As(V) on rare earth oxides [1]. In the pH range of 2.8–11.5, arsenate predominantly exists as $H_2AsO_4^-$ and $HAsO_4^{2-}$ species which is shown in the speciation diagram. Therefore, it can be concluded that these are the major species being adsorbed on the surface of AIAA. The adsorption of As(V) onto AIAA is found to be very high as compared to AA and the suspension pH sets automatically at 7 during the adsorption process which is useful for drinking water systems. Hence further study has been carried out using AIAA as an adsorbent for the removal of As(V).

3.5. Adsorption kinetics

The adsorption kinetics of As(V) on AIAA were examined at different intervals of time. Adsorption takes place rapidly during the first 10–60 min after which it slows down considerably. Maximum adsorption of 99.6% was obtained at 3 h equilibration time. The rate constants of As(V) adsorption were calculated by rate expression of pseudo-first-order and pseudo-second-order models which are given as follows.

Pseudo-first-order rate expression of Lagergen equation [24] is given as

$$\log(q_e - q_t) = \log q_e - k_1 t \quad (3)$$

where q_e and q_t are the amount of arsenate adsorbed in mg/g at equilibrium and at time t (min), respectively, k_1 is the rate constant of the pseudo-first-order adsorption (min^{-1}).

The adsorption rate constant can be determined from the slope of the linear plot of $\log(q_e - q_t)$ versus t (Fig. 4a). k_1 and the correlation coefficient R^2 were found to be 0.003 and 0.6181, respectively which are extremely low indicating that the adsorption of As(V) onto AIAA does not follow first-order rate model.

The pseudo-second-order rate expression is as follows [25]:

$$\frac{t}{q_t} = \frac{1}{k_2 q_e^2} + \frac{t}{q_e} \quad (4)$$

where k_2 is the pseudo-second-order rate constant ($g\,mg^{-1}\,min^{-1}$).

From Eq. (4), k_2 can be calculated from the slope and intercept of the plot t/q_t versus t (Fig. 4b). The value of k_2 and R^2 for the pseudo-second-order rate model is found to be 0.0208 $g\,mg^{-1}\,min^{-1}$ and 0.9994. The low k_2 and high R^2 value suggest that the adsorption is governed by pseudo-second-order model.

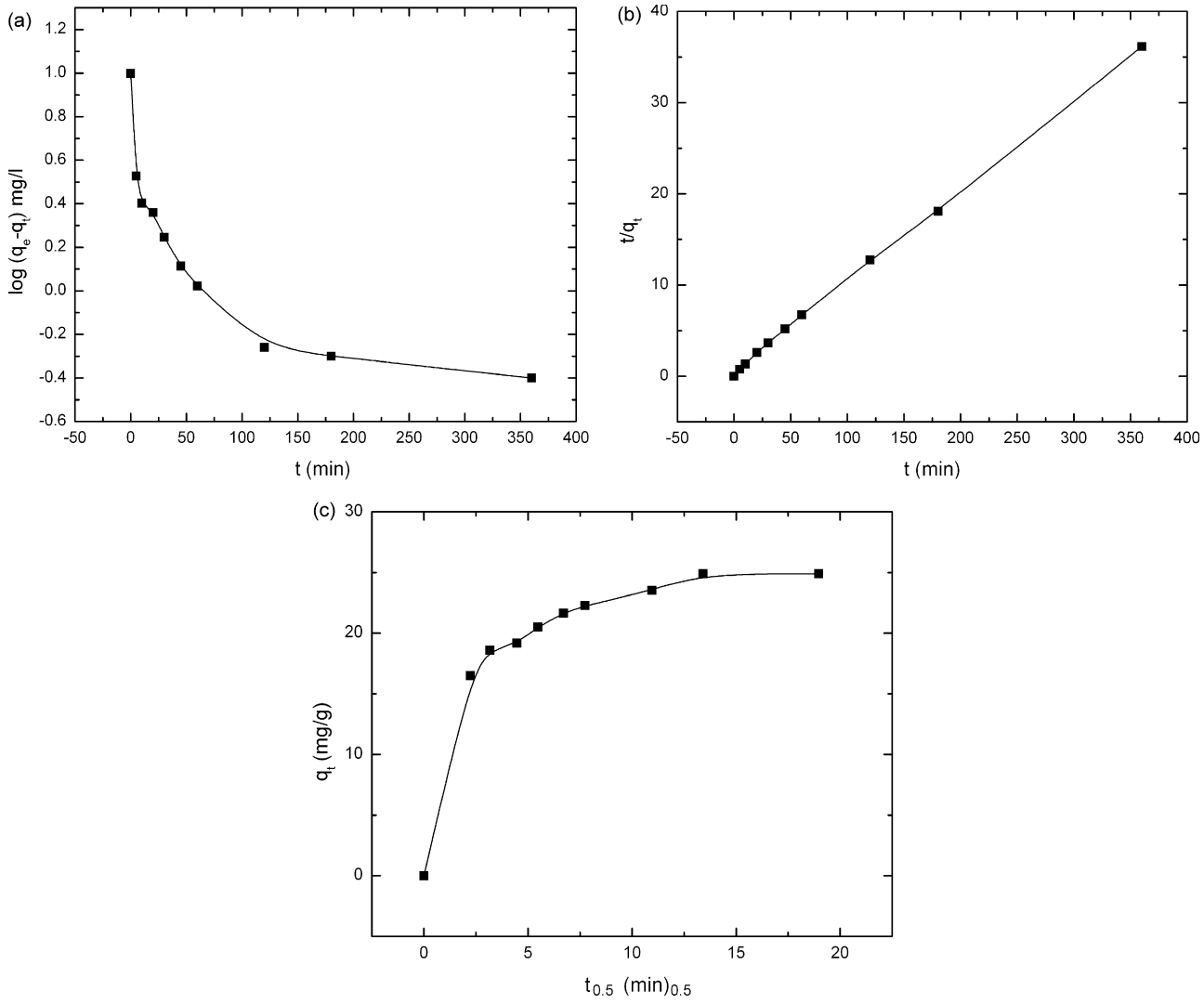

Fig. 4. (a) Pseudo-first-order plot of As(V) adsorption kinetics at pH 7, 8 g/l adsorbent dose and an initial As(V) concentration of 10 mg/l. (b) Pseudo-second-order plot of As(V) adsorption kinetics at pH 7, 8 g/l adsorbent dose and an initial As(V) concentration of 10 mg/l. (c) Intraparticle diffusion plot for adsorption of As(V) at pH 7, 8 g/l adsorbent dose and an initial As(V) concentration of 10 mg/l.

The intraparticle diffusion equation can be described as [26]:

$$q_t = k_i t^{1/2} \tag{5}$$

where k_i is the intraparticle diffusion rate constant (mg g^{-1} min$^{-1/2}$) calculated from Eq. (5).

The plot of q_t versus $t^{1/2}$ (Fig. 4c) shows that the initial curved portion is attributed to the boundary layer diffusion and intraparticle diffusion effect the subsequent linear portion with k_i and R^2 values 0.6949 and 0.9355, respectively. However, as the linear portion of the curve does not pass through the origin, adsorption of As(V) onto AIAA is governed by both surface adsorption as well as intraparticle diffusion effect.

3.6. Effect of adsorbent dose on extent of As(V) adsorption

The variation of As(V) adsorption onto AIAA as a function of adsorbent dose (0.5–16 g/l) at pH 7, 3 h equilibration time and 10 mg/l As(V) concentration is shown in Fig. 5a. It can be observed that adsorption of As(V) increased with increasing adsorbent dose. This might be due to increase in active sites with an increase in amount of adsorbent. The optimum adsorbent dosage required is 8 g/l to reduce up to 40 ppb of As(V) in drinking water.

According to surface sites heterogeneity model, surface hydroxyl groups increase with an increase in adsorbent dose, hence also the binding ability of the surface for an ion, which can be calculated from the distribution coefficient K_D [27]. K_D depends on the pH of the solution and the nature of the adsorbent surface. The K_D value for As(V) on AIAA at pH 7 was calculated by using the following equation:

$$K_D = \frac{C_S}{C_W} (\mathrm{m^3/kg}) \tag{6}$$

where C_S is the concentration of As(V) on the solid particles (mg/kg) and C_W is the equilibrium concentration in water (mg/m^3).

The plot of K_D versus adsorbent dose (Fig. 5b) shows that K_D value increases with increase in AIAA dose up to 8 g/l, which

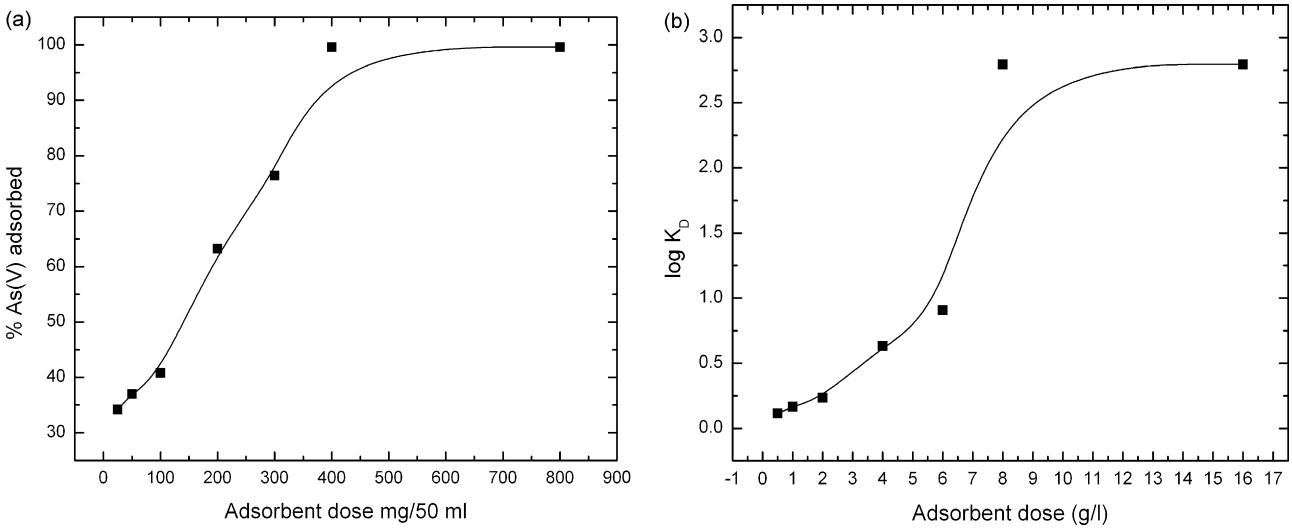

Fig. 5. (a) The plot of percent removal of As(V) as a function of adsorbent dose (g/l) onto AIAA at As(V) concentration 10 mg/l, pH 7 and equilibrium time 3 h. (b) The plot of log K_D value as a function of adsorbent dose (g/l).

implies that the surface of the AIAA is heterogeneous in nature. At higher concentrations, the K_D does not change since the sites available for adsorbing 10 mg/l As(V) are in excess. However at lower concentrations K_D changes and therefore only the initial part of the curve has been considered here.

3.7. Adsorption isotherm

Equilibrium studies were carried out at different concentrations of As(V) (1–25 mg/l) and at three pH values *viz.* 4, 7 and 9 to determine the maximum adsorption capacity of AIAA. Fig. 6a shows that adsorption of As(V) increases with increasing equilibrium concentration at all pH values. At pH 4 and 7, adsorption isotherms are very high and almost same for low As(V) concentration, i.e. up to 10 mg/l which can be confirmed from the effect of pH plot. But for higher concentration of As(V), i.e. >10 mg/l, sorption capacity increases significantly at both the pH values. At pH 9, adsorption increased up to 0.02 m mol/l and then it is spread over a wide concentration range. At pH 7, AIAA successfully removed As(V) to below 40 ppb from water having initial concentration 10 mg/l. A Langmuir isotherm model [28] was correlated to the adsorption isotherm data as follows:

$$\frac{C_e}{X} = \frac{C_e}{X_{max}} + \frac{1}{K_b X_{max}} \quad (7)$$

where C_e is the equilibrium concentration (mmol dm^{-3}), X the amount adsorbed at equilibrium (mmol g^{-1}), K_b and X_{max} are the binding constant and maximum adsorption capacity at a relevant pH, respectively. K_b and X_{max} can be determined from the linear plot of C_e/X versus C_e [Fig. 6b].

At pH 4 and 7, the adsorption isotherm for As(V) fitted satisfactorily to the Langmuir equation. As the adsorption is very low at pH 9, it has not been considered for these calculations. The binding constant and adsorption capacity are found to be 155.42 l/mol and 0.0314 mmol/g, respectively with a correlation coefficient of 0.9589 for pH 4 and 819.54 l/mol

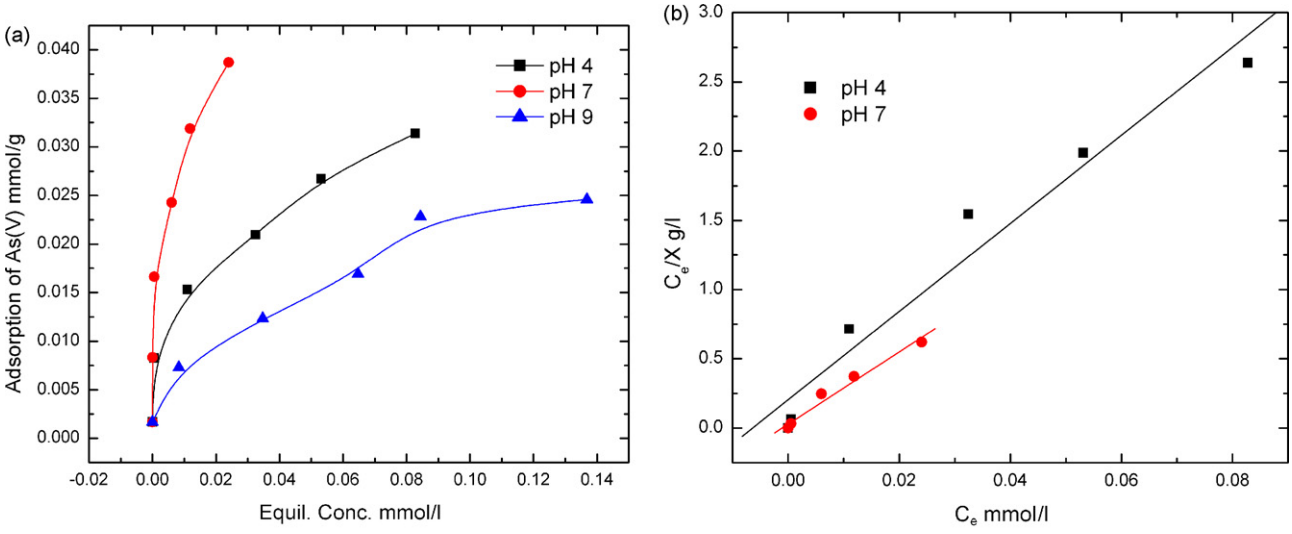

Fig. 6. (a) Adsorption isotherm of As(V) onto AIAA at pH 7, adsorbent dose 8 g/l, equilibrium time 3 h. (b) Langmuir adsorption isotherm of As(V) onto AIAA.

and 0.0401 mmol/g, respectively with a correlation coefficient 0.9747 for pH 7.

In order to predict the favorability of the adsorption process, a dimensionless separation factor or equilibrium parameter R_L, can be calculated using the binding constant K_b obtained from the Langmuirian isotherm model as follows [29]:

$$R_L = \frac{1}{1 + K_b C_0} \quad (8)$$

where C_0 is the initial concentration of As(V) and K_b is the binding constant obtained from the Langmuir isotherm. From the magnitude of the R_L, the adsorption process can be described as $R_L > 1 \Rightarrow$ unfavorable, $R_L = 1 \Rightarrow$ linear, $0 < R_L < 1 \Rightarrow$ favorable, $R_L = 0 \Rightarrow$ irreversible.

The calculated R_L values found in this study are lies in between 0 and 1 for 1–25 mg/l concentration of As(V) in both the pH values, which implies that the As(V) adsorption onto AIAA is a favorable adsorption process.

3.8. Effect of interfering ions

Anions like chloride, nitrate, sulphate, and phosphate present in drinking water may interfere with arsenate ions in the adsorption process and hence the efficiency of the adsorbent is reduced. In order to determine the efficiency of AIAA for removal of As(V) from drinking water, the interference of some common anions such as chloride, nitrate, sulphate and phosphate has been considered. The effect of these anions on adsorption of As(V) (10 mg/l) was studied by varying the concentration of anions from 0 to 100 mg/l individually and in presence of each other. It was observed that the adsorption of As(V) decreased slightly (ca. 3%) in the presence of all the anions except PO_4^{3-}. As(V) adsorption decreases strongly with increasing concentration of PO_4^{3-}. At lower concentration of PO_4^{3-} (25 mg/l), adsorption efficiency of As(V) is lowered by 8% whereas at higher concentration (100 mg/l) it decreases by 27%, which might be due to the competition for the binding sites of the adsorbent between arsenate and PO_4^{3-}.

3.9. Regeneration of the adsorbent

To regenerate the adsorbent, desorption study was carried out at various pH values by appropriate addition of 0.1N HCl and NaOH solution onto As(V) adsorbed AIAA. Initially, desorption of arsenate was difficult in the acidic pH range and there was no leaching of arsenate from the arsenate adsorbed AIAA up

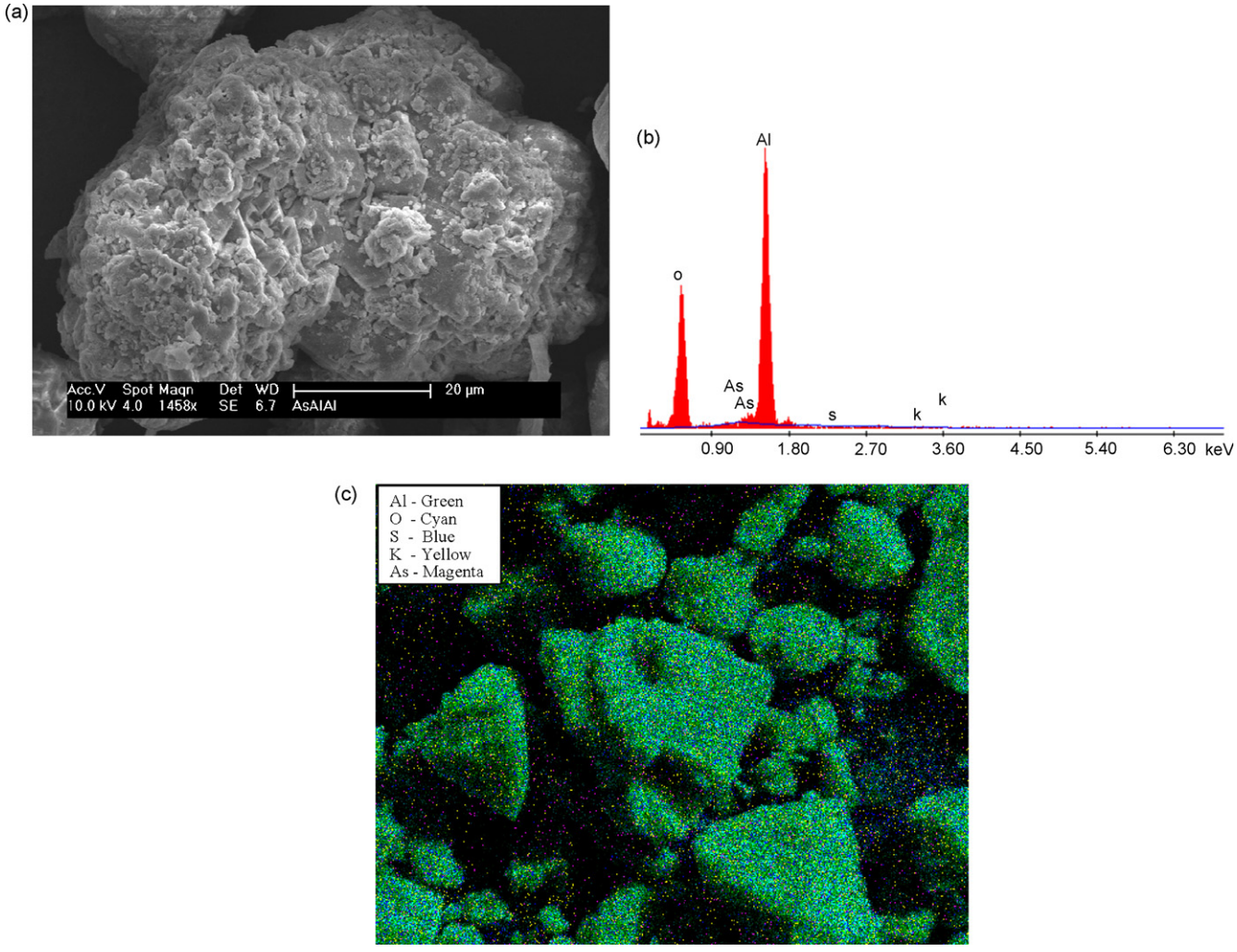

Fig. 7. (a) SEM micrograph, (b) EDAX spectrum and (c) EDAX mapping of arsenic adsorbed alum-impregnated activated alumina.

to pH 8. But, as the pH increases from 9 to 12, desorption of arsenate takes place and complete desorption occurred at pH 12, which is further confirmed from the pH effect result. Adsorption capacity of regenerated AIAA decreases greatly, which shows that impregnation of alum on desorbed AIAA is necessary to further use.

3.10. Zeta potential measurement of As(V) adsorbed AIAA

The IEP value of As(V) adsorbed AIAA was found to be 7.5 (Fig. 1). In the pH range 4–8, arsenic predominantly exists as anionic $H_2AsO_4^-$ and $HAsO_4^{2-}$ species which contribute negative charge on the surface. Therefore, the shift in IEP value to acidic side is due to the formation of negatively charged surface complexes by specific adsorption of $H_xAsO_4^{x-3}$ ions onto AIAA. Further, the shift in IEP value to lower pH range implies that the adsorption of arsenate onto AIAA is through inner-sphere complexes because, in the outer-sphere complexes there is no specific chemical reaction occurs between the adsorbate and the surface that could change the surface charge and the IEP value [30].

3.11. Scanning electron microscopy and EDAX mapping study

Fig. 7a shows the SEM picture of arsenate adsorbed AIAA. From the figure it can be seen that small particles of amorphous precipitate are adhering to the AIAA surface. This might be due to the presence of arsenic on the AIAA surface, which was further confirmed from the EDAX mapping. Fig. 7b shows the presence of a minor peak for As along with major peaks for other elements in the EDAX spectrum. EDAX mapping was carried out for each element and Fig. 7c shows the overlap of Al, O, K, SO_4^{2-} and As. These micrographs provide direct evidence of arsenic adsorption on to AIAA.

4. Conclusions

The alum-impregnated activated alumina was shown to be an effective adsorbent and it could be used for removal of As(V) from drinking water. As(V) was lowered up to 40 ppb when the initial concentration of As(V) in water is 10 mg/l at the optimum pH 7 and 8 g/l adsorbent dose. The adsorption kinetics was found to be fast and maximum adsorption was attained in 60 min time period and followed pseudo-second-order rate law. Intraparticle diffusion study revealed that adsorption of As(V) onto alum-impregnated activated alumina was both by surface adsorption and intraparticle diffusion. Adsorption followed the Langmuir isotherm model for the present system. Interference of the anions shows that PO_4^{3-} experiences the highest competition and retards the adsorption of As(V) onto alum-impregnated activated alumina. Impregnation of alum on desorbed AIAA is necessary to further adsorption of arsenate. Zeta potential measurement, SEM study, EDAX mapping depict the presence of As on the AIAA surface.

Acknowledgements

The authors are thankful to Mr. Kathiravan for his help in carrying out some experimental work. Partial financial assistance from Council of Scientific and Industrial Research, Government of India is gratefully acknowledged.

References

[1] A.M. Raichur, V. Panvekar, Removal of As(V) by adsorption onto mixed rare earth oxides, Sep. Sci. Technol. 37 (5) (2002) 1095–1108.
[2] S. Goldberg, Competitive adsorption of arsenate and arsenite on oxides and clay minerals, Soil Sci. Soc. Am. J. 66 (2) (2002) 413–421.
[3] R. Mamtaz, D.H. Bache, Reduction of arsenic in groundwater by coprecipitation with iron, J. Water Supply (2001) 313–324.
[4] M.-J. Kim, Separation of inorganic arsenic species in groundwater using ion exchange methods, Bull Environ. Contam. Toxicol. 67 (1) (2001) 46–51.
[5] R.C. Cheng, H.C. Wang, M.D. Beuhler, Enhanced coagulation for arsenic removal, J. Am. Water Works Assoc. 86 (9) (1994) 79–90.
[6] L. Cumbal, A.K. Sengupta, Arsenic removal using polymer-supported hydrated iron(III) oxide nanoparticles: role of Donnan membrane effect, Environ. Sci. Technol. 39 (2005) 6508–6515.
[7] V.Y. Pokonova, Carbon adsorbents for the sorption of arsenic, Carbon 36 (4) (1998) 457–459.
[8] M.P. Elizalde, J. Mattusch, W.D. Einicke, R. Wennrich, Sorption on natural solids for arsenic removal, Chem. Eng. J. 81 (1–3) (2001) 187–195.
[9] E. Diamopoulos, S. Ioannidis, G.P. Sakellaropoulos, As(V) removal from aqueous solutions by fly ash, Water Res. 27 (12) (1993) 1773–1777.
[10] K.S. Subramanian, T. Viraraghavan, T. Phommanrong, S. Tanjore, Manganese greensand for removal of arsenic in drinking water, Water Quality Res. J. Can. 32 (3) (1997) 551–561.
[11] M. Badruzzamana, P. Westerhoffa, R.U.K. Detlef, Intraparticle diffusion and adsorption of arsenate onto granular ferric hydroxide (GFH), Water Res. 38 (2004) 4002–4012.
[12] M.M. Gosh, J.R. Yaun, Environ. Prog. 5 (1987) 150.
[13] T.S. Singh, K.K. Pant, Equilibrium, kinetics and thermodynamic studies for adsorption of As(III) on activated alumina, Sep. Purif. Technol. 36 (2004) 139–147.
[14] T.-F. Lin, J.-K. Wu, Adsorption of arsenite and arsenate within activated alumina grains: equilibrium and kinetics, Water Res. 35 (2001) 2049–2057.
[15] B.E. Reed, R. Vaughan, L. Jiang, As(III), As(V), Hg and Pb removal by Fe-oxide impregnated activated carbon, J. Environ. Eng. 126 (2000) 869–873.
[16] C.H. Lai, S.L. Lo, C.F. Lin, Water Sci. Technol. 30 (1994) 175.
[17] J.G. Huang, J.C. Liu, Enhanced removal of As(V) from water with iron coated spent catalyst, Sep. Sci. Technol. 32 (9) (1997) 1557–1569.
[18] O.S. Thrunavukkarasu, T. Viraraghavan, K.S. Subramanian, Removal of arsenic in drinking water by iron oxide-coated sand and ferrihydrite-batch studies, Water Quality Res. J. Can. 36 (2001) 55–70.
[19] R.L. Vaughan, B.E. Reed, Modelling As(V) removal by a iron oxide impregnated activated carbon using the surface complexation approach, Water Res. 39 (2005) 1005–1014.
[20] M.L. Ballinas, E. Rodriguez de San Miguel, M.T. De Jesus Rodriguez, O. Silva, M. Munoz, J. De Gyves, Arsenic(V) removal with polymer inclusion membranes from sulfuric acid media using DBBP as carrier, Environ. Sci. Technol. 38 (3) (2004) 886–891.
[21] S.A. Wasay, Md.J. Haron, S. Tokunaga, Adsorption of fluoride, phosphate and arsenate ions on lanthanum impregnated silica gel, Water Environ. Res. 68 (1996) 295.
[22] I.A. Katsoyiannis, A.I. Zouboulis, Removal of arsenic from contaminated water sources by sorption onto iron-oxide-coated polymeric materials, Water Res. 36 (2002) 5141–5155.

[23] S.S. Tripathy, J.L. Bersillon, K. Gopal, Removal of fluoride from drinking water by adsorption onto alum-impregnated activated alumina, Sep. Purif. Technol. 50 (2006) 310–317.
[24] M.S. Chiou, H.Y. Li, Adsorption behavior of reactive dye in aqueous solution on chemical cross-linked chitosan beads, Chemosphere 50 (2003) 1095–1105.
[25] G. McKay, Y.S. Ho, Pseudo-second-order model for sorption processes, Process Biochem. 34 (1999) 451–465.
[26] C. Namasivayam, R.T. Yamuna, Adsorption of direct red 12 B by biogas residual slurry: equilibrium and rate processes, Environ. Pollut. 89 (1995) 1–7.
[27] L. Sigg, in: W. Stumm (Ed.), Aquatic Surface Chemistry: Chemical processes at the particle-water interface, John Wiley and Sons, New York, 1987, p. 319.
[28] T. Balaji, H. Matsunaga, Adsorption characteristics of As(III) and As(V) with titanium dioxide loaded amberlite XAD-7 resin, Anal. Sci. 18 (2002) 1345–1349.
[29] G. McKay, H.S. Blair, J.R. Garden, Adsorption of dyes on chitin 1. Equilibrium studies, J. Appl. Polym. Sci. 27 (8) (1982) 3043–3057.
[30] W. Stumm, Chemistry of the Solid–Water Interface, Wiley–Interscience, New York, 1999.